HHS Public Access

Author manuscript

J Immunol. Author manuscript; available in PMC 2016 October 01.

Published in final edited form as:

J Immunol. 2015 October 1; 195(7): 3237–3247. doi:10.4049/jimmunol.1402701.

Decreased T_{FR}/T_{FH} ratio in SIV-infected rhesus macaques may contribute to accumulation of T_{FH} cells in chronic infection

Ankita Chowdhury[*], **Perla Maria Estrada Del Rio**[*,†], **Greg K Tharp**[*], **Ronald P Trible**[*], **Rama R Amara**[*], **Ann Chahroudi**[‡], **Gustavo Reyes-Teran**[†], **Steven E. Bosinger**[*], and **Guido Silvestri**[*]

[*]Emory Vaccine Center and Yerkes National Primate Research Center, Emory University, Atlanta, GA

[†]Departamento de Investigación en Enfermedades Infecciosas, Instituto Nacional de Enfermedades Respiratorias, “Ismael Cosio Villegas”. México D.F., México

[‡]Department of Pediatrics, Emory University School of Medicine, Atlanta, GA

Abstract

T follicular helper cells (T_{FH}) are critical for the development and maintenance of germinal centers (GC) and humoral immune responses. During chronic HIV/SIV infection T_{FH} accumulate, possibly as a result of antigen persistence. The HIV/SIV-associated T_{FH} expansion may also reflect lack of regulation by suppressive follicular regulatory $CD4^+$ T-cells (T_{FR}). T_{FR} are natural regulatory T-cells (T_{REG}) that migrate into the follicle and, similarly to T_{FH}, up-regulate CXCR5, Bcl-6, and PD1. Here we identified T_{FR} as $CD4^+CD25^+FoxP3^+CXCR5^+PD1^{hi}Bcl\text{-}6^+$ within lymph nodes of rhesus macaques (RM) and confirmed their localization within the GC by immunohistochemistry. RNA sequencing showed that T_{FR} exhibit a distinct transcriptional profile with shared features of both T_{FH} and T_{REG}, including intermediate expression of FoxP3, Bcl-6, PRDM1, IL-10, and IL-21. In healthy, SIV-uninfected RM, we observed a negative correlation between frequencies of T_{FR} and both T_{FH} and GC B-cells as well as levels of $CD4^+$ T-cell proliferation. Following SIV infection, the T_{FR}/T_{FH} ratio was reduced with no change in the frequency of T_{REG} or T_{FR} within the total $CD4^+$ T-cell pool. Finally, we examined whether higher levels of direct virus infection of T_{FR} were responsible for their relative depletion post-SIV infection. We found that T_{FH}, T_{FR} and T_{REG} sorted from SIV- infected RM harbor comparable levels of cell-associated viral DNA. Our data suggests that T_{FR} may contribute to the regulation and proliferation of T_{FH} and GC B-cells *in vivo* and that a decreased T_{FR}/T_{FH} ratio in chronic SIV infection may lead to unchecked expansion of both T_{FH} and GC B-cells.

Introduction

Several key findings over the past few years have energized efforts towards the development of an effective HIV vaccine, including the discovery and characterization of a number of

Corresponding Address: Dr. Guido Silvestri, Division of Microbiology and Immunology, Yerkes National Primate Research Center, Department of Pathology & Laboratory Medicine, Emory University School of Medicine, 929 Gatewood Rd, Atlanta, GA 30329, gsilves@emory.edu phone: 404-727-7217 fax: 404-727-7768.

broadly neutralizing antibodies (bnAbs) that develop in a subset of HIV-infected individuals. However, the mechanisms involved in shaping antibody responses to immunization with HIV antigens or natural HIV infection, including the generation of bnAbs remain incompletely understood (1). Importantly, HIV-Env-specific bnAbs develop at relatively late stages of HIV infection, and show peculiar genetic and molecular features, including a high level of divergence from germ line predecessors, which indicates that they are the products of extensive somatic hyper-mutation within germinal centers (GCs), as well as the presence of unusually long CDR3 regions (2). Perplexingly, there appear to be no direct or predictable routes to the development of these bnAbs from the germ line predecessors, and it remains unclear whether this process is driven by antigenic mutations and/or escape as opposed to specific intrinsic aspects of the B-cell or T-helper cell response (3). A better understanding of the mechanisms responsible for the development of bnAbs is crucial to harness this type of immunity for HIV prevention and therapy in humans.

T follicular helper cells (T_{FH}) are critical for the development and maintenance of GCs and competition for survival signals from T_{FH} via molecules such as CD40L and IL-21 is thought to be a key mechanism of selection of high affinity B-cells (4). The regulation of T_{FH} frequency, and by extension the regulation of their impact on GC B-cell development and function, is vital to the quality of the humoral immune response (5). While the presence of too few T_{FH} may lead to abortive GC formation and defective B-cell responses, an over-expansion was found to be associated with the prevalence of autoantibodies (6, 7). It is possible that an expansion of T_{FH} also lowers the selection pressure on GC B-cells and leads to the emergence of low-affinity B-cells (8).

Several studies have shown that T_{FH} accumulate during the chronic stages of HIV/SIV infection. This accumulation occurs even though these cells support high levels of viral replication and represent an important component of the persistent virus reservoir under anti-retroviral therapy (9). The chronic expansion of T_{FH} in the case of HIV/SIV infection with persistent virus replication may be a direct result of antigenic persistence. As expected, HIV/SIV-associated expansion of T_{FH} is associated with dysregulation of B-cell responses with ineffective memory cell formation and hyper-gammaglobulinemia (10),(11). Whether and to what extent this T_{FH} expansion is also related to a deficit in the physiologic regulation of specific T_{FH} immune response within the lymph nodes remains unknown. However, this possibility would be consistent with the well-known observation that the chronic phase of pathogenic HIV/SIV infections is associated with a state of generalized immune activation that is resistant to the normal mechanisms of immune regulation.

Under normal circumstances, regulation of T_{FH} function is mediated at least in part by a recently described subset of $CD4^+$ T-cells termed T follicular regulatory (T_{FR}) cells. T_{FR} are thought to develop from natural regulatory T-cells (T_{REG}) that express lineage-associated markers such as FoxP3, CD25, as well as low levels of CD127. These T_{FR} migrate into the follicles and GCs of lymph nodes by virtue of their expression of CXCR5 (and down-modulation of CCR7) and, similarly to T_{FH}, express high levels of Bcl-6 and PD1 (12) (13). Of note, the role of T_{FR} in the immuno-pathogenesis of HIV/SIV infections is currently unknown, both in terms of ability to negatively regulate HIV-specific B-cell responses (including, potentially, the production of bnAbs) and to suppress local virus-induced

immune activation. Indeed, none of the previous reports on T_{FH} dynamics in the context of SIV or HIV infection have distinguished between cells that either do or do not co-express T_{REG}-associated markers. Thus the T_{FR} subset within the broader $CXCR5^+Bcl\text{-}6^+PD1^+$ is not fully characterized in the setting of HIV/SIV infection.

In this study, we described and characterized phenotypically, histologically, and genomically a T_{FR} population that is found within the GCs of rhesus macaques (RM) and express markers associated with both T_{FH} and T_{REG} cells. The hypothesis that T_{FR} play a suppressive role *in vivo* is supported by the observation that their frequency is inversely correlated with both the levels of T_{FH} and GC B-cells and the percentage of proliferating $CD4^+$ T-cells. In the setting of SIV infection, we found that T_{FR} show a slow *in vivo* proliferative response after the initial infection and exhibit only a small increase in their frequency within the total $CD4^+$ T-cell pool during the chronic phase. In conjunction with the large expansion of T_{FH} observed following SIV infection, this phenomenon leads to a significantly decreased T_{FR}/T_{FH} ratio in the lymph nodes of chronically SIV-infected RM. These data may suggest that, during SIV infection, a lack of T_{FR} expansion may allow for a progressive accumulation of T_{FH} cells in the lymph nodes of chronically infected RM, thus indirectly contributing to the aberrant immune activation that characterizes this pathogenic infection.

Materials and Methods

Animals

The study involved a total of 40 Indian origin female rhesus macaques (RM) divided as follows: (i) Ten healthy, unvaccinated and SIV-uninfected RM; (ii) Ten healthy, SIV-immunized but SIV-uninfected RM; (iii) Eleven unvaccinated SIV-infected animals; and (iv) Nine vaccinated and SIV-infected RM. Animals were vaccinated with a SIVmac239 Gag-, Pol-, and Env-expressing DNA vaccine with inactivating mutations in proteases, half of which also co-expressed GM-CSF. These were followed by two boosts of a SIVmac239 Gag-, Pol-, and Env-expressing MVA vaccine as described previously (14). All infections were a result of SIVsmE660 intra-vaginal challenge at 2.06×10^4 $TCID_{50}$ grown in RM peripheral blood mononuclear cells (PBMC). Lymph node biopsies were collected for measurement of a number of immunological parameters at day -35 prior to infection and days 14 and 168 after infection (i.e., acute and chronic phase, respectively). Spleen and lymph nodes were collected at necropsies performed at six months post infection. All animals were housed at Yerkes National Primate Center at Emory University and were cared for in accordance with National Institute of Health guidelines and following protocols approved by the Institutional Animal Care and Use Committee.

Tissue processing

Lymphocytes were isolated from freshly obtained lymph node and spleens by passing homogenized tissue through a 70-μm cell strainer and lysing blood cells with ACK Lysis buffer. Tissue collection was performed as previously described (15). Cells to be later used for sorting were cryopreserved at −80 degrees C in FBS media containing 10% DMSO.

Immunophenotyping and flow cytometry

Multi-color flow cytometric analysis was performed on mononuclear cells isolated from blood and lymph nodes according to standard procedures using monoclonal antibodies directed against RM markers and human markers that also cross-react with the same markers in RM. For optimum staining of intra-cellular markers, permeabilization of cells using the eBioscience FoxP3-permeabalization buffer was performed as recommended by the manufacturers. Pre-determined optimal concentrations of the following antibodies and reagents were used: CD3-Alexa700 (clone SP34-2), CD4-Allophycocyanin-Cy7 (clone OKT-4), Bcl-6-PeTexasRed (clone K112-91), Ki67- FITC (clone B56), CCR5-PE (clone 3A9), CTLA4- BV421 (clone BNI3) from BD, CXCR5-PerCP eFlour 710 (clone MU5BEE), PD1-PeCy7 (clone J105), CD127-PeCy5 (clone eBio-RDR5) from eBioscience and CD20-BV650 or PE-CF594 (clone 2H7), CD25-BV711 (clone BC96), Helios-FITC (clone 22F6) and FoxP3-Allophycocyanin (clone 150D) from Biolegend, and Live/Dead Fixable Aqua from Invitrogen. Flow cytometric data were acquired using LSRII flow cytometer using BD's FACS DiVA software. Acquired data were analyzed using Flow Jo version9.3.2 following the gating strategy described in Figure1. Further analyses were performed using PRISM (GraphPad) and Excel (Microsoft Office 2011) software.

Cell Sorting

Cryopreserved cells were thawed in a 37 degree C water bath and rested overnight for 8-10 hours and then stained for sorting. Splenocytes from 5 SIV-uninfected and vaccinated RM as well as 9 unvaccinated SIV-infected animals were used for sorting of T_{FH}, T_{FR}, and T_{REG}. Cell populations were sorted using FACS Aria II flow cytometer. Cells were first gated based on light scatter followed by positive gating on cells negative for Live/Dead Fixable Aqua and positive for CD3 and CD4. After collecting bulk $CD4^+$ cells the following three populations were collected: T_{FR} ($CXCR5^+PD1^{hi}CD127^-CD25^+$), T_{FH} ($CXCR5^+PD1^{hi}CD127^{+/-}CD25^-$) and T_{REG} ($CXCR5^{+/-}PD1^{lo/int}CD127^-CD25^+$).

Immunohistochemistry and Confocal Microscopy

Immunohistochemstry was performed on 5-μm tissue sections mounted on glass-slides, which were deparaffinized and rehydrated with double-distilled H_2O. Antigen retrieval was performed in 1xDako Target Retrieval Solution (pH 6.0) in a pressure cooker heating slides to 122 degrees C for 30s. Slides were then rinsed in ddH_2O and incubated for 10 minutes using Dako Protein block. Slides were then incubated with rabbit anti-(1:200), mouse anti-FoxP3 (1:100) and goat anti-PD1 (1:500) for 1 hour at room temperature. Next, slides were washed in TBS with 0.05% Tween-20. Slides were then incubated for an hour in the dark with secondary antibody cocktail containing donkey anti-rabbit Alexa 488 (1:500), donkey anti-mouse Alexa-594 (1:500) and donkey anti-goat Alexa 647 (1:500). After washing in TBS with 0.05% Tween-20, Prolong Gold with DAPI was applied to all the slides. Confocal microscope images were obtained using Olympus FV10i® Confocal Microscope with CellSens® 1.9 Digital Imaging software.

Quantitative PCR for SIV gag DNA

Cell-associated viral DNA was measured in sorted cell populations from RM lymph nodes by RT-PCR as previously described(16-18).

RNA-Seq Library Preparation

Total RNA was prepared using the QIAGEN RNEasy Micro Kit. Libraries were generated using the CLONTECH SMARTer HV kit, barcoding and sequencing primers were added using NexteraXT DNA kit. Libraries were validated by microelectrophoresis, quantified, pooled and clustered on Illumina TruSeq v3 flowcell. Clustered flowcell was sequenced on an Illumina HiSeq 1000 in 100-base single-read reactions.

RNA-Seq Data Analysis

RNA-Seq data were submitted to the GEO repository at the National Center for Biotechnology Information (NCBI). RNA-Seq data were aligned to a provisional assembly of Indian Macaca mulatta (MaSuRCA rhesus assembly v.7_20130927) using STAR version 2.3.0e (19) (20). Transcripts were annotated using the provisional UNMC annotation v7.6. Transcript assembly, abundance estimates, and differential expression analysis was performed using Cufflinks v2.1.1 and Cuffdiff (21). All samples had read counts > 12000000 and unique mapping percentages in the range of 63 – 76 %; no samples were excluded from the analysis for technical issues. Differentially expressed genes were defined by pair-wise comparison of each phenotype. Differential gene lists were uploaded to Ingenuity Pathway Analysis software (v1.0 Ingenuity Systems, http://www.ingenuity.com/) and pathways with significant enrichment by Fisher's Exact test and the Benjamini-Hochberg multiple testing correction. Heat maps and other visualization were generated using Partek Genomics Suite v6.6. RNA-seq data is publically available at the GEO repositories (accession number: GSE69756, URL: http://www.ncbi.nlm.nih.gov/geo/query/acc.cgi?acc=GSE69756).

RT-PCR validation of RNA sequencing data

Total RNA was prepared using the QIAGEN RNEasy Micro Kit from sorted T_{FR}, T_{FH} and T_{REG} cells. RNA quantity was measured using Nanodrop analysis and reverse transcribed as previously described for RNA sequencing. Finally, 0.1 μl of cDNA was used for real time SYBR green PCR analysis using an ABI 7900 HT Real-time PCR instrument (Applied Biosystems). Primer sequences for PCR were GAPDH: Fwd5′-GCACCACCAACTGCTTAGCAC-3′, Rev 5′- TCTTCTGGGTGGCAGTGATG-3′. IL2RA: Fwd5′- GGCTTCATTTTCCCACGGT-3′, Rev 5′- GCAGCTGGCGGACCAA-3′. IL6R: Fwd5′- TTCGGCCGGACTGTTCTG-3′, Rev 5′- GCACCCCATCTCCGACG-3′. SLAMF6: Fwd5′- TGG AAC ATC TCT TGC CTT CAT AG-3′, Rev 5′- GTT GCT GAG TTT CAG GGA GTA G-3′. SAP/SH2D1A: Fwd5′- CTC TGC AGT ATC CAG TTG AGA AG-3′, Rev 5′- GGC TTT CAG GCA GAC ATC A-3′. XIAP: Fwd 5′- GAG GAA CCC TGC CAT GTA TAG-3′, Rev 5′- GTG TAG TAG AGT CCA GCA CTT G-3′; PRDM1: Fwd 5′- TGT GGT ATT GTC GGG ACT TTG-3′, Rev 5′- GCT TGA GAT TGC TCT GTG TTT G-3′; CCL20: Fwd 5′- GCA ACT TTG ACT GCT GTC TTC-3′, Rev 5′- CAG CAT TGA TGT CAC AGG TTT C-3′; PD1: Fwd 5′- TCCTTGGCCACTGGTGTTC-3′, Rev 5′-

CTTCTCCTGAGGGAAGGAGC-3′; IL10: Fwd 5′- AAGACCCTCAGGCTGAGGCT-3′, Rev 5′- TCCACGGCCTTGCTCTTG-3′; IL21: Fwd 5′- TGTGAATGACTTGGACCCTGAA-3′, Rev 5′AAACAGGAAATAGCTGACCACTCA-3′. Relative RNA transcript levels were calculated normalized to primer efficiency and housekeeping gene RNA (GAPDH).

Statistical Analyses

Except for RNA sequencing data, all statistical analyses were conducted using GraphPad Prism 5.0. Comparisons of mean fluorescence intensity between cell populations in uninfected RM were made using Wilcoxon signed rank tests (Fig 2). Man-Whitney U tests were used to compare frequencies of populations in uninfected, acutely infected and chronically infected RM (Figure 4, 5). Spearman rank correlation tests were used to analyze all correlations (Figure 6). All p values less than 0.05 were defined as significant.

Results

T_{FR} are distinct from T_{FH} and T_{REG} and can be found within lymph node GCs in RM

Recent studies of GC T_{FH} have defined these cells based on their surface expression of the chemokine receptor CXCR5 and very high levels of the co-inhibitory receptor PD1 (10). However, a fraction of these canonically defined T_{FH} also express the lineage-specific T_{REG} marker FoxP3 and have been therefore defined as T_{FR} as proposed in (22-24). Here we identified $CD4^+$ T_{FR} by flow cytometry by their co-expression of CXCR5, PD1, FoxP3 and CD25 within lymph nodes of uninfected RM. The gating strategy used to define T_{FH}, T_{FR}, and T_{REG} throughout this study is shown in Figure 1A. Of note, the gating strategy for T_{REG} cells includes both $CXCR5^+$ and $CXCR5^-$ cells. To confirm the presence of T_{FR} within GCs we conducted an immuno-histochemistry (IHC) analysis. As shown in Figure 1B, single cells with nuclear expression for FoxP3 and surface expression of and PD1 were identified with GCs of uninfected RM. These T_{FR} can also be readily identified within GCs of SIV-infected RM (Fig 1C). Interestingly, several *bonafide* T_{REG}, identified by their expression of FoxP3 and but not PD1, are visible in the T-cell zone just outside the GC (Fig 1C). Presumably, some of these T_{REG} migrate into the GC and up-regulate T_{FH}-like markers along their differentiation pathway to T_{FR}. Figure 1C also shows that, as expected, non-FoxP3 expressing “true” T_{FH} are also seen within GCs of the same animals.

T_{FR} express markers of both T_{FH} and T_{REG} differentiation

We next performed a comprehensive examination of the T_{FR} phenotype in healthy, SIV-uninfected RM. As shown in Figure 2, our analysis of relative mean fluorescence intensities (MFI) for T_{FR} markers confirmed that T_{FR} express FoxP3 and CD25 at comparable levels to T_{REG} (Figure 2A) and both CXCR5 and PD1 at comparable levels to T_{FH} (Figure 2B). We next examined in T_{FR} the expression patterns of a series of markers (i.e., CD127, CTLA4, Bcl-6, and Helios) that have been linked to either T_{FH} or T_{REG} phenotype and function (1, 25). CD127, the IL-7 receptor α-chain, is expressed at low levels on T_{REG} in humans (26), (27) (28). As expected, we find that T_{FR} express CD127 at lower levels than the bulk of $CD4^+$ T-cells, and similar or even lower levels than those observed in T_{REG} and T_{FH} (Figure 2C). CTLA4 is a key negative T-cell regulator that is constitutively expressed on T_{REG} and,

upon ligation, induces down-modulation of cytokine production and inhibition of cell-cycle progression (25). Consistent with previous reports in murine models (12), we observed that T_{FR} express CTLA4 at a higher frequency and MFI than both T_{REG} and T_{FH} cell populations (Figure 2D), consistent with a putative role of T_{FR} as negative regulators of GC responses. Helios is a transcription factor expressed in thymus-derived natural T_{REG} cells (29). As shown in Figure 2F, T_{FR} express Helios at levels that are even higher than those observed in T_{REG} in terms of both frequency of positive cells and MFI, thus suggesting that T_{FR} originate from natural T_{REG} in RM as well as in mice.

Transcriptome analysis of T_{FR} reveals a distinct but overlapping transcriptional profile compared to T_{FH} and T_{REG}

To further define the functional features of T_{FR} in RM, we next examined the transcriptional profiles of T_{FH}, T_{FR} and T_{REG} using RNA-Seq by Illumina technology. Splenocytes from five healthy, SIV-uninfected and unvaccinated RM were sorted into "bulk" $CD3^+CD4^+$ T-cells, T_{REG}, T_{FH} and T_{FR} based on the following phenotypic markers: T_{FR} ($CXCR5^+PD1^{hi}CD127^-CD25^+$), T_{FH} ($CXCR5^+PD1^{hi}CD127^{+/-}CD25^-$) and T_{REG} ($CXCR5^{+/-}PD1^{lo/int}CD127^-CD25^+$). In mice, T_{FR} are derived from thymic T_{REG} precursors and acquire homing markers that allow them to traffic to GCs, while maintaining a transcriptome and suppressive function that most closely resembles T_{REG} (12, 13). To examine the transcriptional profile of T_{FR} relative to T_{REG} and T_{FH} in healthy, SIV-uninfected RM, we first performed principal component analysis (PCA) on a subset of the most highly expressed transcripts detected in T_{FH}, T_{REG} and T_{FR} (Figure 3A). The transcriptomes of each subset were clearly distinct and grouped by subset, with T_{REG} displaying the highest degree of intra-subset variability, and T_{FH} and T_{FR} subsets being more tightly distributed. We next compared the expression of several canonical T_{FH} and T_{REG} transcripts between the three subsets. As shown in Figure 3B-D, T_{FH}- and T_{REG}-related genes showed expression patterns that behaved as predicted with genes such as IL-10 expressed in T_{FR} and T_{REG} but absent in T_{FH}. Importantly, RNA sequencing data confirmed that T_{FR} share expression of T_{REG} signature transcripts such as FoxP3, GZMB, PRDM1 and IL2RA (Figure 3A). However, we found that several other T_{REG}-specific transcripts were expressed at lower levels in T_{FR} than in T_{REG}, including TRAF6, CD74, CCL20 and IL1R1. Similar to previous studies in mice, T_{FR} also showed elevated expression of the prototypical T_{FH} genes CXCR5, PD1/PDCD1, BCL-6, CXCL13, and ICOS. In fact, T_{FR} demonstrated a peculiarly high expression of the T_{FH} and T_{REG}-specific genes Bcl-6 and FoxP3, respectively. Interestingly, for several genes (SH2D1A/SAP, IL-21, CXCR5, IL-10) gene expression was higher in T_{FR} than either T_{REG} or T_{FH}, thus suggesting that the $CD25^+CXR5^+PD1^{hi}$ phenotype may represent a more transcriptionally active population than classical T_{REG} or T_{FH}. This latter set of RNA-sequencing data provides strong evidence that T_{FR} are indeed a distinct cell subset and that the somewhat hybrid transcriptional profile of T_{FR} is not simply due to the sample being a mixture of T_{REG} and T_{FH}. Of note, elevated expression of IL-10 in T_{FR} compared to T_{REG} has been previously reported in murine studies (13).

To then compare the profile of gene expression between T_{FR} with T_{REG} and T_{FH} subsets without using any *a priori* information, we defined T_{FH} and T_{REG} expression signatures by

statistically contrasting RNA-sequencing data from T_{FH} and T_{REG} with bulk $CD4^+$ T-cells. After exclusion of transcripts that had zero expression in any of the populations, a total of 88 genes made up the combined T_{FH} and T_{REG} signature of which 12 genes were T_{REG} related. Many, but not all, canonical T_{REG} and T_{FH} genes were also identified as significantly upregulated compared to bulk $CD4^+$ T-cells. The lack of statistical significance for some prototypical transcripts is likely due to the presence T_{REG} and T_{FH} subsets within the bulk $CD4^+$ population used as a comparator sample. Nevertheless, we found that T_{FR} cells show similar levels of expression of T_{FH} signature genes such as Bcl-6, TIGIT, CD200, LAT and BATF (Figure 3C). T_{FR} cells also express mRNA for key T_{FH}-related genes that are important for B-cell help, including IL-21, SH2D1A, CD40L and CD84. One notable difference between our data in RM and previously published mouse studies is that we observed high expression of IL-21 in T_{FR}, suggesting that these cells have acquired some specific genomic and functional features in primates. As shown in Supplementary Figure 2A-C, the expression patterns of IL-21, SH2D1A, SLAMF6, PD1, IL6R, CCL20, IL2RA, IL10, PRDM1, and XIAP were confirmed by RT-PCR quantification. In addiction, levels of protein expression of IL-21 by T_{FR} , T_{FH}, and T_{REG} were also measured by flow cytometry and further confirmed the pattern observed by RNA sequencing and RT-PCR (Supplementary Figure 2D).

SIV infection is associated with a decrease in the T_{FR}/T_{FH} ratio

The dynamics of T_{FR} in the setting of HIV or SIV infection have not been previously investigated, and in fact all published studies of T_{FH} dynamics during HIV/SIV infection used a definition of these cells that included T_{FR} as well. To study the kinetics of T_{FR}, T_{FH}, and T_{REG} following SIV infection of RM we measured the frequency of these cells within the lymph nodes prior to infection, 2 weeks post infection and 6 months post infection with SIVsmE660. The RM included in these kinetics analyses included both unvaccinated as well as animals that were challenged following immunization with a SIVmac239 Gag-, Pol-, and Env-expressing DNA vaccine (with or without GM-CSF) followed by two boosts of a SIV239 Gag-, Pol-, and Env-expressing MVA vaccine. As previously reported, we found a significant increase ($p<0.0001$) in frequency of T_{FH} at 24 weeks post infection (Figure 4A). Interestingly, the frequency of T_{FR} measured as percent of total $CD4^+$ T-cells also showed a significant ($p=0.0001$) increase during chronic SIV infection (Figure 4A). However, when the frequency of T_{FR} is measured as percentage of total T_{FH}, we found that the T_{FR} decrease significantly at both the acute ($p=0.0385$) and chronic ($p=0.0016$) stages of SIV infection (Figure 4B). Accordingly, the overall ratio of T_{FR} to T_{FH} cells also decreased significantly ($p=0.0018$) at the week 24 post-infection time point as compared to baseline (Figure 4C). The increase of both T_{FH} and T_{FR} as a percent of $CD4^+$ T-cells after infection is likely the result of proliferation driven by antigen-persistence as well as virus-mediated depletion of other $CD4^+$ T-cell subsets. However, the relative decrease in the frequency of T_{FR} when measured as percentage of T_{FH} suggests that the low frequency of these regulatory cells might contribute to the expansion and accumulation of T_{FH} in chronically SIV-infected RM. Of note, we found no significant changes in T_{REG} frequencies after SIV infection within the lymph nodes. To better define the kinetics of T_{FH} and T_{FR} during SIV infection we next measured the level of cell proliferation using the well-established marker Ki67. We observed that T_{FH} show a significant increase in proliferating cells during the acute

($p<0.0001$) phase and chronic ($p=0.0001$) phase of infection (Figure 4D). T_{FR} have a similar pattern of proliferation, with a significant increase in proliferating cells during the acute ($p<0.0001$) phase and chronic ($p=0.0376$) phase of infection (Figure 4D). In contrast, the level of Ki67 expression in T_{REG} remains relatively low throughout our analysis with a small significant increase ($p=0.0141$) during the chronic phase of infection (Figure 4D).

Similar levels of SIV infection of T_{FR} as compared to T_{FH} and T_{REG} despite higher CCR5 expression

Several studies have shown that, during HIV and SIV infection, T_{FH} are highly infected with the virus despite their relative increase within the total $CD4^+$ T-cell pool (9). While the actual *in vivo* lifespan of T_{FH}, either infected or uninfected, remains unknown in the setting of HIV/SIV infection, the presence of a notable fraction of these cells expressing the proliferation marker Ki67 suggests that their number could be maintained through continual replenishing from precursors located outside the GC. To measure the level of direct SIV infection of T_{FR}, T_{FH}, and T_{REG} we sorted these subpopulations from the lymph nodes of a subset of our studied animals and quantified the levels of total cell-associated SIV-DNA by RT-PCR. This analysis revealed that T_{FH}, T_{FR} and T_{REG} derived from chronically SIV-infected RM all harbor comparably high levels of cell-associated viral DNA (Figure 5A). Interestingly, the levels of SIV infection were similarly high between T_{FR} and T_{FH} even though the surface expression levels of the main SIV co-receptor CCR5 were significantly higher in T_{FR} as compared to T_{FH} (Figure 5B).

The frequency of T_{FR} is negatively correlated with the number and proliferation of both T_{FH} and GC B-cells

To further examine the relationship between T_{FR} and T_{FH} and GC B-cells we next performed a set of correlation analyses in the RM included in this study, both SIV-infected and uninfected. We first observed that, in healthy uninfected RM, the frequency of T_{FR} (as fraction of the total T_{FH} pool) is negatively correlated with the percentages of T_{FH} (as fraction of total $CD4^+$ T-cells) and GC B-cells (as fraction of total B-cells) (Figure 6A). In addition, we found that, in the same animals, the frequency of T_{FR} (as fraction of T_{FH}) is negatively correlated with the level of $CD4^+$ T-cell proliferation as measured by Ki67 expression (Figure 6A).

We next performed the same correlation analyses in our cohort of SIV-infected RM. The SIV-infected RM included in these regression analyses included both unvaccinated as well as animals that were challenged following immunization with a SIVmac239 Gag-, Pol-, and Env-expressing DNA vaccine (with or without GM-CSF) followed by two boosts of a SIV239 Gag-, Pol-, and Env-expressing MVA vaccine. In the SIV- infected RM, similar to what was observed in uninfected animals, the frequency of T_{FR} (as fraction of T_{FH}) is negatively correlated with the percentages of both T_{FH} and GC B-cells (Figure 6B). However, the negative correlation between frequency of T_{FR} (as fraction of T_{FH}) and the level of $CD4^+$ T-cell proliferation as measured by Ki67 expression is not seen in SIV-infected RM (Figure 6B). The negative correlation between T_{FR} cells (as a frequency of T_{FH} cells) and both T_{FH} and GC B-cell frequencies is consistent with the hypothesis that T_{FR}

cells play a role in regulating T_{FH} and GC responses under normal circumstances and in the setting of chronic SIV infection.

Comparative analysis of the T_{FR} transcriptome in SIV-infected and uninfected RM

To further define the effect of SIV infection on T_{FR}, we next compared the transcription profiles of T_{FR} that were isolated from unvaccinated chronically SIV-infected and uninfected RM (Fig. 7). We performed RNA-Seq analysis and transcripts that were significantly differentially expressed in T_{FR} sorted from SIV infected vs. uninfected RM were analyzed by Ingenuity Pathway Analysis. Unsurprisingly, a large proportion of genes induced during SIV infection in T_{FR} (CD3G, FOS, CD4, ZAP70, PIK3CD, STAT3) were components of T-cell proliferation, activation of T-cell effector function, and co-stimulatory activation (data not shown). The enhanced T-cell activation was consistent with our observation that T_{FR} cells express higher levels of the proliferation marker Ki67 compared to T_{REG} (Figure 4D). We also observed that several genes implicated in pathways regulating apoptosis or cell cycle control were perturbed in SIV-infected RMs. Of particular interest was the observation that the pro-apoptotic gene FASLG was >100-fold induced, while the anti-apoptotic regulator XIAP was significantly down-regulated. This latter finding was again validated by RT-PCR (Supplementary Figure 2B). Thus, while we observed a significant increase of the proliferation marker Ki67 in T_{FR} after SIV infection (Figure 4D), a pro-apoptotic shift of gene expression may explain why only a modest increase in T_{FR} frequency was observed (Figure 4A).

T_{FH} require IL-6 signaling and STAT3 expression for differentiation and, once mature, produce several factors that support B-cell activation. Conversely, IL-2 receptor signaling drives STAT5 to activate Blimp1/PRDM1, which ultimately blocks T_{FH} differentiation (30). However, T_{FR} express both Blimp/PRDM1 and Bcl-6. Here we find that both IL-6 and IL-2 signaling genes are enriched in T_{FR} after SIV infection. However, several of these genes, such as MAPK1, are common to different cytokine signaling pathways, thus making it difficult to establish if SIV infection causes a shift in the T_{FR}/T_{FH} differentiation pressure. Interestingly, downstream signaling for IL-10, a regulatory cytokine produced by both T_{FR} and T_{REG}, is also enriched in T_{FR} post infection. Additionally, ICOS-ICOSL signaling was also enriched in T_{FR} post infection. These data suggest that T_{FR} may be engaged in similar T_{FH}-like cell-surface receptor-ligand interactions with B-cells. In addition to genes that were identified with differential expression without any *a priori* knowledge, we also examined genes with known function in T_{FR} and T_{REG}. After infection, T_{FR} cells show a significant increase in the expression of PD1, IL6R, SLAMF6 and CD84, i.e., all markers associated with T_{FH} differentiation and function (Figure 7B). We also found a significant decrease in STAT3 and IL2RA in T_{FR} after SIV infection and a non-significant decrease in Bcl-6 expression. Finally, as expected, we also observed several other changes in expression patterns of the T_{FH} and T_{FR} signature gene sets as we had previously determined (Supplementary Figure 1). Overall, these data indicate a complex remodeling of gene expression in T_{FR} following SIV infection of RM.

Discussion

T_{FH} cells are critical to the development of the humoral response to infections, and their role in the setting of HIV and SIV infection (and vaccination) is the subject of intense investigation. However, some aspects of the complex T_{FH} response to HIV/SIV infection remain poorly understood, including (i) their role in promoting the development of broadly neutralizing HIV/SIV-specific antibodies, and (ii) their role in the immunopathogenesis of the infection. In particular, the mechanisms by which T_{FH} accumulate during the chronic stage of infection despite high levels of direct virus infection are unclear. Importantly, a series of recent studies have shown that T_{FH} include a subset of cells that are derived from thymic T_{REG} precursors, express the classical T_{REG} markers (i.e., FoxP3 and CD25 as well as low levels of CD127), and acquire T_{FH} markers (i.e., PD1, CXCR5, and Bcl-6) while migrating into the GC of lymph nodes, where they are thought to act as regulators of the host humoral immune response. To the best of our knowledge this study-- together with the independently generated set of data that are included in the accompanying manuscript by the group of Dr. Franchini and Dr. Vaccari -- represents the first description of the main features of T_{FR} in a non-human primate species. In this work we also investigated the dynamics of this cell subset during SIV infection of rhesus macaque (RM).

The main findings of the current study are the following: (i) T_{FR} show distinct yet overlapping phenotype as compared to T_{FH} and T_{REG} based on a combination of flow cytometric, histological, and transcriptional analyses; (ii) in healthy, SIV-uninfected RM, the frequencies of T_{FR} are negatively correlated with the levels of both T_{FH} and GC B-cells; (iii) following SIV infection, the T_{FR}/T_{FH} ratio is reduced; and (iv) T_{FR} sorted from SIV-infected RM harbor comparable levels of cell-associated viral DNA as compared to T_{FH} and T_{REG}. Collectively, these data indicate that while T_{FR} closely resemble T_{FH} in several biological aspects, they are also clearly distinguishable from this cell subset in terms of both their immunophenotype and transcriptional profile. It is therefore important that, in future studies of T_{FH}, a distinction be made between T_{FR} and true, "non-T_{FR}" T_{FH} to fully take into account the complexity of the different $CD4^+$ T-cell subsets that are present in the GC of lymph nodes.

The observation that T_{FR} express proteins typically expressed by T_{FH}, such as CD40L, as well as proteins typically expressed by T_{REG}, like IL-10 and CTLA4, is consistent with studies in mice showing that T_{FR} are thymic-derived T regulatory (nT_{REG}) cells that migrate into the follicle and, in a manner similar to T_{FH}, up-regulate CXCR5, Bcl-6 and PD1 in a B-cell dependent manner (24). The production of IL-21 by T_{FR} cells is an intriguing new finding and suggests that T_{FR} play a more complex role in RMs than has been described in mice. In addition, PCA suggests that the transcriptional profile of T_{FR} tend to be more similar to T_{FH} than T_{REG}. Further studies are required to fully investigate the functional role played by T_{FR} in RMs and, specifically, in the context of SIV infection. The finding that over 90% of T_{FR} express Helios as measured by flow cytometry is also consistent with the nT_{REG} origin of these cells. Importantly, these immunophenotypic and RNA sequencing data were complemented by histological analyses showing that T_{FR} are found within GCs of both uninfected and infected RM. While $CD4^+FoxP3^+$ T_{REG} were found in abundance outside the GC, $CD4^+PD1^+T_{FH}$ and $CD4^+PD1^+FoxP3^+T_{FR}$ were both only seen within the

GC. The hypothesis that T_{FR} play an immune regulatory role *in vivo* is supported by the observation that their frequency is inversely correlated with both the levels of T_{FH} and GC B-cells. These data are consistent with mouse studies indicating that (i) T_{FR} suppress T_{FH} *in vitro* and prevent the outgrowth of non-antigen specific B-cells (13), and that (ii) T_{FR} may inhibit antibody production without an effect on T-cell activation, thus indicating an ability to directly regulate B-cells(31).

In the setting of *in vivo* SIV infection, we found that T_{FR} exhibited only a small increase in their frequency within the total $CD4^+$ T-cell pool. In conjunction with the large expansion of T_{FH} that is consistently observed following SIV infection, the minor expansion of T_{FR} leads to a significantly decreased T_{FR}/T_{FH} ratio in the lymph nodes of chronically SIV-infected RM. We confirmed this trend in the ratio of T_{FR}/T_{FH} cells after SIV infection by quantifying the number of T_{FH} and T_{FR} cells by immunohistochemistry (Supplementary Table 1). While the current set of results does not allow us to determine whether and to what extent the kinetics of T_{FH} and T_{FR} during SIV infection are mechanistically linked, it is conceivable that the limited T_{FR} expansion facilitates progressive accumulation of T_{FH} in chronically SIV-infected RM, thus indirectly contributing to the aberrant immune activation that characterizes this pathogenic infection. On the other hand, it is also possible that the strong proliferation of T_{FH} and associated increase in PD1 expression following SIV infection hampers the development or differentiation of T_{FR} as suggested (31).

Comparison of the transcriptional profiles of T_{FR} cells pre and post-SIV infection showed a significant up-regulation of transcripts typically expressed by activated T_{REG} including FOSB, FABP5, USP2 and USP13 (data not shown) (32), thus suggesting that T_{FR} may be involved in the generalized immune activation associated with pathogenic SIV infection. Interestingly, we also observed a down regulation of several T_{FH} and T_{REG} signature genes as established by our own algorithm. This somewhat unexpected observation indicates that SIV infection has a complex effect on the in vivo phenotype and function of T_{FR}. A better understanding of the overall contribution of T_{FR} to the immunopathogenesis of AIDS, in terms of causing either the virus-associated B-cell dysfunction or the changes in the lymph node architecture and function, will require further in vitro and in vivo investigation of the suppressive effect by these T_{FR} on the function of either T_{FH} or GC B-cells.

While $CD4^+$ T-cells are the main target for HIV and SIV infection, substantial difference exist between various $CD4^+$ T-cell subsets in terms of their relative levels of direct virus infection *in vivo* (33-35). In this study we tested the possibility that the decrease in the T_{FR}/T_{FH} ratio observed during SIV infection of RM was associated with higher level of virus infection in T_{FR} as compared to T_{FH}. However, our comparative analysis of the cell-associated viral burdens in sorted T_{FR}, T_{FH}, and T_{REG} revealed similar levels of SIV-DNA in the three $CD4^+$ T-cell subsets, even though T_{FR} exhibited higher levels of the SIV co-receptor CCR5 as compared to the other two subsets.

In summary, the presented data provide the first comprehensive description of T_{FR} in healthy, uninfected RM, as well as the first examination of the kinetics of these cells in the setting of pathogenic SIV infection. These results support the hypothesis that these cells play an important immune regulatory role *in vivo*, and that a relative decline of the T_{FR}/T_{FH} ratio

may be involved in establishing a state of chronic immune activation in the B-cell areas of lymph nodes during pathogenic HIV and SIV infection.

Supplementary Material

Refer to Web version on PubMed Central for supplementary material.

Acknowledgements

We would like to thank Dr. Barbara Cervasi and Dr. Kiran Gill at the Flow Cytometry Core at Emory Vaccine Center and Dr. Prachi Sharma and Dr. Deepa Kodandera at the Molecular Pathology Core Lab. We would also like to thank the animal care and veterinary staff at the Yerkes National Primate Research Center.

This work was supported by National Institutes of Health Grant U19 AI096187, RR000165/OD011132 to the Yerkes National Primate Research Center and P30 AI050409 to the Emory Center for AIDS Research.

References

1. Pissani F, Streeck H. Emerging concepts on T follicular helper cell dynamics in HIV infection. Trends in immunology. 2014; 35:278–286. [PubMed: 24703588]
2. Corti D, Lanzavecchia A. Broadly neutralizing antiviral antibodies. Annual review of immunology. 2013; 31:705–742.
3. Murphy MK, Yue L, Pan R, Boliar S, Sethi A, Tian J, Pfafferot K, Karita E, Allen SA, Cormier E, Goepfert PA, Borrow P, Robinson JE, Gnanakaran S, Hunter E, Kong XP, Derdeyn CA. Viral escape from neutralizing antibodies in early subtype A HIV-1 infection drives an increase in autologous neutralization breadth. PLoS pathogens. 2013; 9:e1003173. [PubMed: 23468623]
4. Crotty S. Follicular helper CD4 T cells (TFH). Annual review of immunology. 2011; 29:621–663.
5. Pratama A, Vinuesa CG. Control of TFH cell numbers: why and how? Immunology and cell biology. 2014; 92:40–48. [PubMed: 24189162]
6. Yang X, Yang J, Chu Y, Xue Y, Xuan D, Zheng S, Zou H. T follicular helper cells and regulatory B cells dynamics in systemic lupus erythematosus. PloS one. 2014; 9:e88441. [PubMed: 24551101]
7. Ma CS, Deenick EK. Human T follicular helper (Tfh) cells and disease. Immunology and cell biology. 2014; 92:64–71. [PubMed: 24145858]
8. Vinuesa CG. HIV and T follicular helper cells: a dangerous relationship. The Journal of clinical investigation. 2012; 122:3059–3062. [PubMed: 22922252]
9. Perreau M, Savoye AL, De Crignis E, Corpataux JM, Cubas R, Haddad EK, De Leval L, Graziosi C, Pantaleo G. Follicular helper T cells serve as the major CD4 T cell compartment for HIV-1 infection, replication, and production. The Journal of experimental medicine. 2013; 210:143–156. [PubMed: 23254284]
10. Lindqvist M, van Lunzen J, Soghoian DZ, Kuhl BD, Ranasinghe S, Kranias G, Flanders MD, Cutler S, Yudanin N, Muller MI, Davis I, Farber D, Hartjen P, Haag F, Alter G, Schulze zur Wiesch J, Streeck H. Expansion of HIV-specific T follicular helper cells in chronic HIV infection. The Journal of clinical investigation. 2012; 122:3271–3280. [PubMed: 22922259]
11. Petrovas C, Koup RA. T follicular helper cells and HIV/SIV-specific antibody responses. Current opinion in HIV and AIDS. 2014; 9:235–241. [PubMed: 24670319]
12. Chung Y, Tanaka S, Chu F, Nurieva RI, Martinez GJ, Rawal S, Wang YH, Lim H, Reynolds JM, Zhou XH, Fan HM, Liu ZM, Neelapu SS, Dong C. Follicular regulatory T cells expressing Foxp3 and Bcl-6 suppress germinal center reactions. Nature medicine. 2011; 17:983–988.
13. Linterman MA, Pierson W, Lee SK, Kallies A, Kawamoto S, Rayner TF, Srivastava M, Divekar DP, Beaton L, Hogan JJ, Fagarasan S, Liston A, Smith KG, Vinuesa CG. Foxp3+ follicular regulatory T cells control the germinal center response. Nature medicine. 2011; 17:975–982.
14. Lai L, Kwa S, Kozlowski PA, Montefiori DC, Ferrari G, Johnson WE, Hirsch V, Villinger F, Chennareddi L, Earl PL, Moss B, Amara RR, Robinson HL. Prevention of infection by a granulocyte-macrophage colony-stimulating factor co-expressing DNA/modified vaccinia Ankara

simian immunodeficiency virus vaccine. The Journal of infectious diseases. 2011; 204:164–173. [PubMed: 21628671]

15. Ortiz AM, Klatt NR, Li B, Yi Y, Tabb B, Hao XP, Sternberg L, Lawson B, Carnathan PM, Cramer EM, Engram JC, Little DM, Ryzhova E, Gonzalez-Scarano F, Paiardini M, Ansari AA, Ratcliffe S, Else JG, Brenchley JM, Collman RG, Estes JD, Derdeyn CA, Silvestri G. Depletion of CD4(+) T cells abrogates post-peak decline of viremia in SIV-infected rhesus macaques. The Journal of clinical investigation. 2011; 121:4433–4445. [PubMed: 22005304]
16. Cartwright EK, McGary CS, Cervasi B, Micci L, Lawson B, Elliott ST, Collman RG, Bosinger SE, Paiardini M, Vanderford TH, Chahroudi A, Silvestri G. Divergent CD4+ T memory stem cell dynamics in pathogenic and nonpathogenic simian immunodeficiency virus infections. Journal of immunology. 2014; 192:4666–4673.
17. Vanderford TH, Slichter C, Rogers KA, Lawson BO, Obaede R, Else J, Villinger F, Bosinger SE, Silvestri G. Treatment of SIV-infected sooty mangabeys with a type-I IFN agonist results in decreased virus replication without inducing hyperimmune activation. Blood. 2012; 119:5750–5757. [PubMed: 22550346]
18. Klatt NR, Shudo E, Ortiz AM, Engram JC, Paiardini M, Lawson B, Miller MD, Else J, Pandrea I, Estes JD, Apetrei C, Schmitz JE, Ribeiro RM, Perelson AS, Silvestri G. CD8+ lymphocytes control viral replication in SIVmac239-infected rhesus macaques without decreasing the lifespan of productively infected cells. PLoS pathogens. 2010; 6:e1000747. [PubMed: 20126441]
19. Sandler NG, Bosinger SE, Estes JD, Zhu RT, Tharp GK, Boritz E, Levin D, Wijeyesinghe S, Makamdop KN, del Prete GQ, Hill BJ, Timmer JK, Reiss E, Yarden G, Darko S, Contijoch E, Todd JP, Silvestri G, Nason M, Norgren RB Jr. Keele BF, Rao S, Langer JA, Lifson JD, Schreiber G, Douek DC. Type I interferon responses in rhesus macaques prevent SIV infection and slow disease progression. Nature. 2014; 511:601–605. [PubMed: 25043006]
20. Dobin A, Davis CA, Schlesinger F, Drenkow J, Zaleski C, Jha S, Batut P, Chaisson M, Gingeras TR. STAR: ultrafast universal RNA-seq aligner. Bioinformatics. 2013; 29:15–21. [PubMed: 23104886]
21. Trapnell C, Hendrickson DG, Sauvageau M, Goff L, Rinn JL, Pachter L. Differential analysis of gene regulation at transcript resolution with RNA-seq. Nature biotechnology. 2013; 31:46–53.
22. Vinuesa CG, Cyster JG. How T cells earn the follicular rite of passage. Immunity. 2011; 35:671–680. [PubMed: 22118524]
23. Alexander CM, Tygrett LT, Boyden AW, Wolniak KL, Legge KL, Waldschmidt TJ. T regulatory cells participate in the control of germinal centre reactions. Immunology. 2011; 133:452–468. [PubMed: 21635248]
24. Wollenberg I, Agua-Doce A, Hernandez A, Almeida C, Oliveira VG, Faro J, Graca L. Regulation of the germinal center reaction by Foxp3+ follicular regulatory T cells. Journal of immunology. 2011; 187:4553–4560.
25. Wing JB, Sakaguchi S. Foxp3(+) T(reg) cells in humoral immunity. International immunology. 2014; 26:61–69. [PubMed: 24324208]
26. Liu W, Putnam AL, Xu-Yu Z, Szot GL, Lee MR, Zhu S, Gottlieb PA, Kapranov P, Gingeras TR, Fazekas de St Groth B, Clayberger C, Soper DM, Ziegler SF, Bluestone JA. CD127 expression inversely correlates with FoxP3 and suppressive function of human CD4+ T reg cells. The Journal of experimental medicine. 2006; 203:1701–1711. [PubMed: 16818678]
27. Seddiki N, Santner-Nanan B, Martinson J, Zaunders J, Sasson S, Landay A, Solomon M, Selby W, Alexander SI, Nanan R, Kelleher A, Fazekas de St Groth B. Expression of interleukin (IL)-2 and IL-7 receptors discriminates between human regulatory and activated T cells. The Journal of experimental medicine. 2006; 203:1693–1700. [PubMed: 16818676]
28. Dunham RM, Cervasi B, Brenchley JM, Albrecht H, Weintrob A, Sumpter B, Engram J, Gordon S, Klatt NR, Frank I, Sodora DL, Douek DC, Paiardini M, Silvestri G. CD127 and CD25 expression defines CD4+ T cell subsets that are differentially depleted during HIV infection. Journal of immunology. 2008; 180:5582–5592.
29. Getnet D, Grosso JF, Goldberg MV, Harris TJ, Yen HR, Bruno TC, Durham NM, Hipkiss EL, Pyle KJ, Wada S, Pan F, Pardoll DM, Drake CG. A role for the transcription factor Helios in human CD4(+)CD25(+) regulatory T cells. Molecular immunology. 2010; 47:1595–1600. [PubMed: 20226531]

30. Ray JP, Marshall HD, Laidlaw BJ, Staron MM, Kaech SM, Craft J. Transcription factor STAT3 and type I interferons are corepressive insulators for differentiation of follicular helper and T helper 1 cells. Immunity. 2014; 40:367–377. [PubMed: 24631156]

31. Sage PT, Francisco LM, Carman CV, Sharpe AH. The receptor PD-1 controls follicular regulatory T cells in the lymph nodes and blood. Nature immunology. 2013; 14:152–161. [PubMed: 23242415]

32. Birzele F, Fauti T, Stahl H, Lenter MC, Simon E, Knebel D, Weith A, Hildebrandt T, Mennerich D. Next-generation insights into regulatory T cells: expression profiling and FoxP3 occupancy in Human. Nucleic acids research. 2011; 39:7946–7960. [PubMed: 21729870]

33. Moreno-Fernandez ME, Zapata W, Blackard JT, Franchini G, Chougnet CA. Human regulatory T cells are targets for human immunodeficiency Virus (HIV) infection, and their susceptibility differs depending on the HIV type 1 strain. Journal of virology. 2009; 83:12925–12933. [PubMed: 19828616]

34. Brenchley JM, Hill BJ, Ambrozak DR, Price DA, Guenaga FJ, Casazza JP, Kuruppu J, Yazdani J, Migueles SA, Connors M, Roederer M, Douek DC, Koup RA. T-cell subsets that harbor human immunodeficiency virus (HIV) in vivo: implications for HIV pathogenesis. Journal of virology. 2004; 78:1160–1168. [PubMed: 14722271]

35. Brenchley JM, Vinton C, Tabb B, Hao XP, Connick E, Paiardini M, Lifson JD, Silvestri G, Estes JD. Differential infection patterns of CD4+ T cells and lymphoid tissue viral burden distinguish progressive and nonprogressive lentiviral infections. Blood. 2012; 120:4172–4181. [PubMed: 22990012]

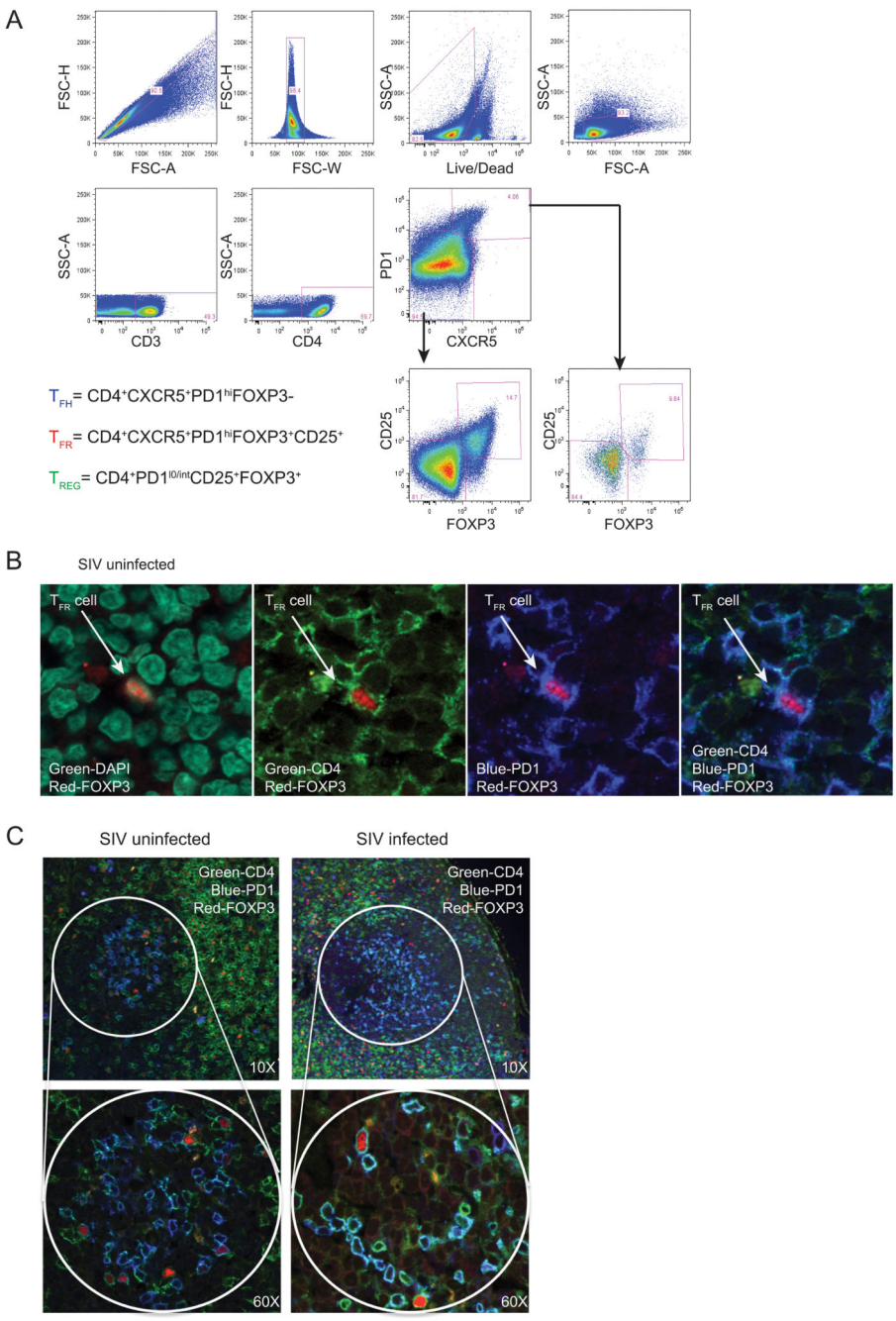

Figure 1. T_{FR} can be defined by flow cytometry and identified by confocal microscopy within the germinal centers of RM

(A) Representative flow cytometry plot of lymphocytes from lymph nodes of untreated uninfected RM showing the gating strategy used to define T_{FR}, T_{FH} and T_{REG} cell populations. (B) Representative confocal microscope image showing a single T_{FR} within the lymph node of an uninfected RM. The first image shows staining for DAPI (green) and FoxP3 (red). The second image shows the same section with CD4 (green) and FoxP3 (red), the third PD1 (blue) and FoxP3 (red) and the last image CD4 (green), PD1 (blue) and FoxP3 (red). (C) Representative images of lymph node biopsies from SIV uninfected and acutely

infected RM showing cells stained with CD4 (green), FoxP3 (red) and PD1 (blue) within the GC regions.

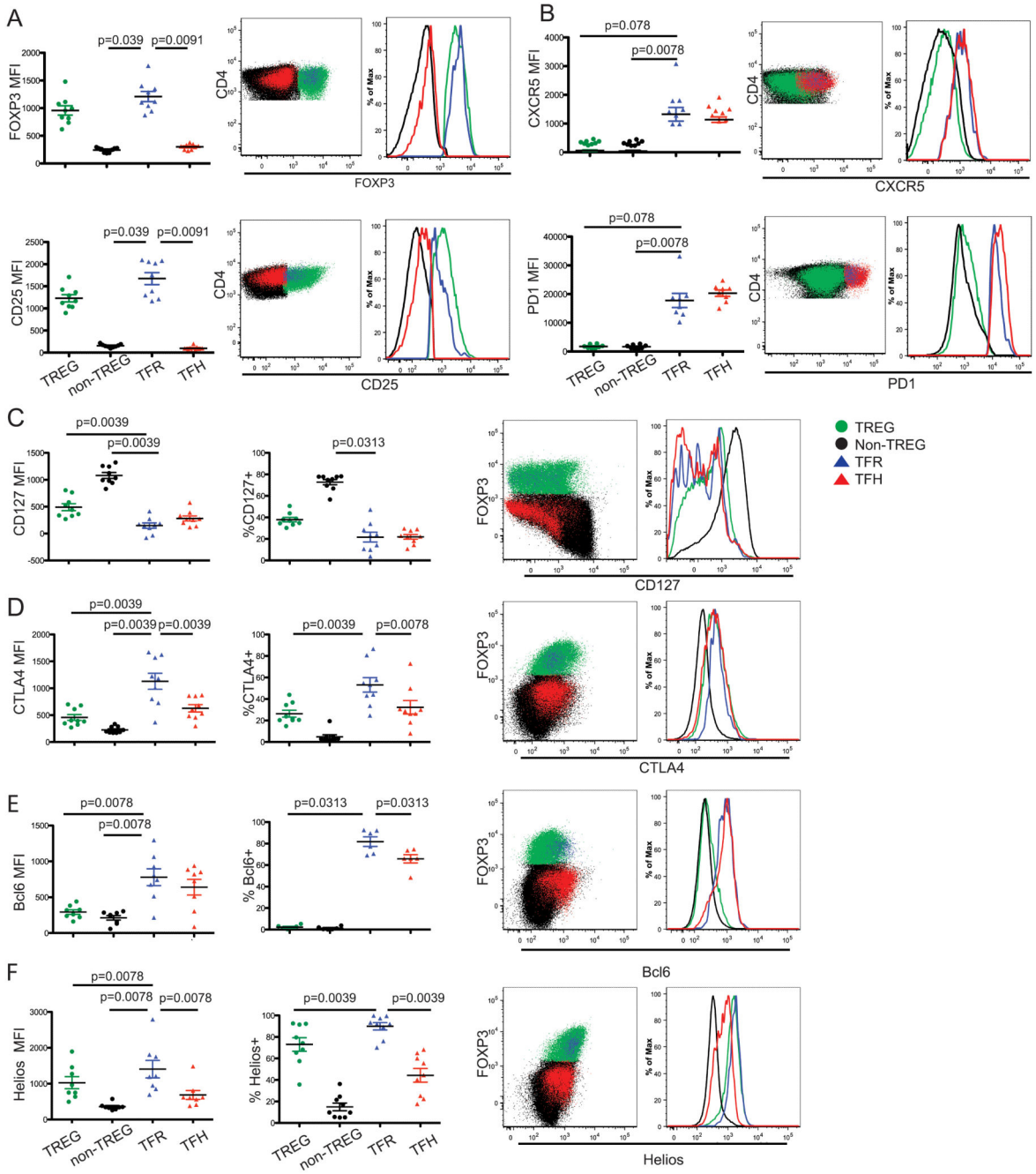

Figure 2. T_{FR} share immunophenotypical features of both T_{FH} and T_{REG} populations

Mean fluorescence intensity, percent positive, representative flow cytometry plots and histograms (Panels A, B, C, D, E, F) for expression of various immunophenotypical markers (i.e., FoxP3, CD25, CXCR5, PD-1, CD127, CTLA4, Bcl-6 and Helios) among T_{REG}, non-T_{REG}, T_{FR} and T_{FH} populations from LN of healthy, unvaccinated and uninfected RM. Non-T_{REG} here are defined as all $CD4^{+}CD25^{-}FoxP3^{-}$ T-cells. Significance was determined by Wilcoxon signed rank tests.

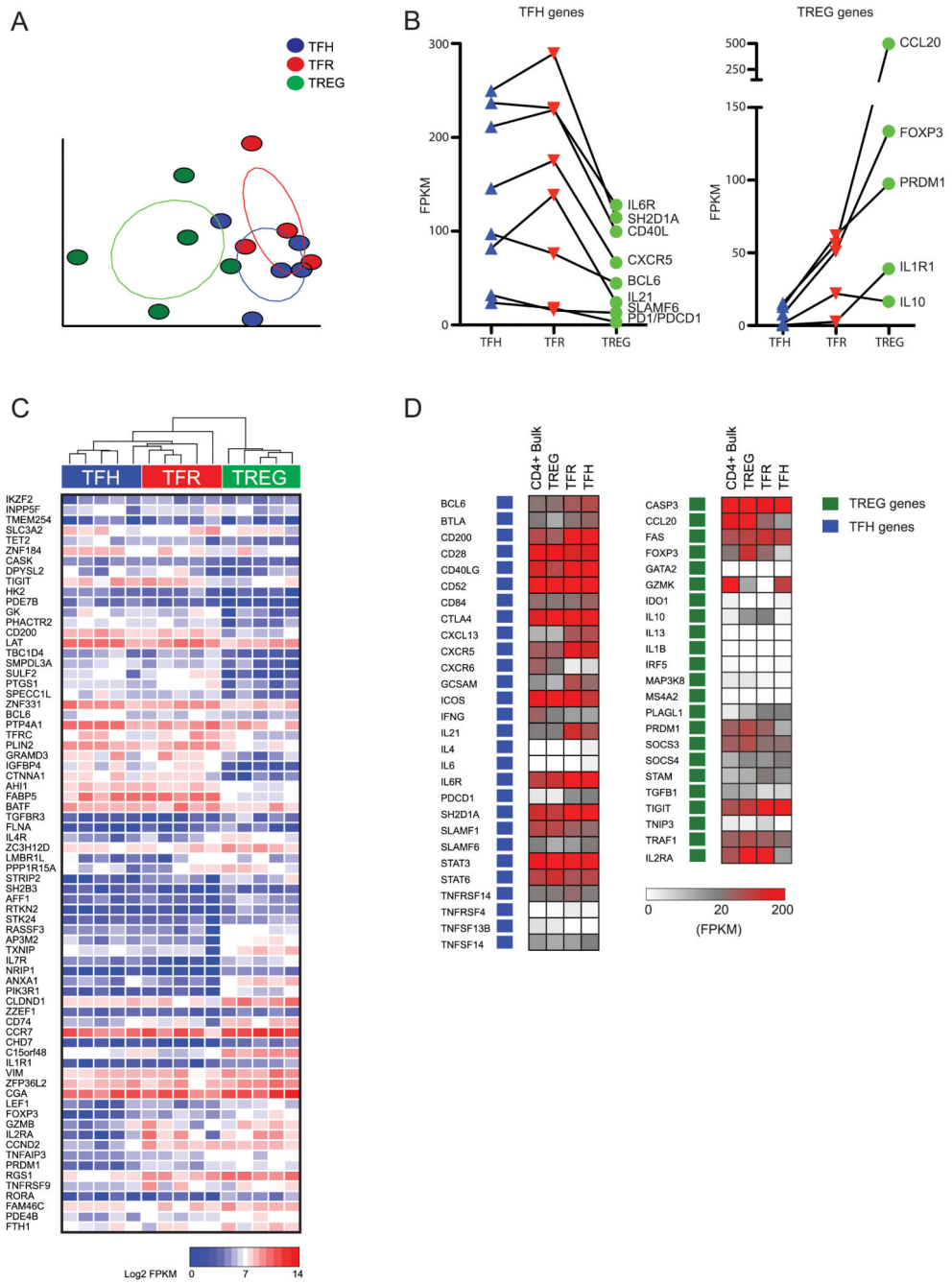

Figure 3. RNA expression patterns confirm that T_{FR} share T_{FH} and T_{REG} like phenotype

(A) Principal components analysis of RNA transcripts from five healthy, SIV-uninfected RM. Each circle represents the transcriptome of a sorted population of T_{FH} (blue), T_{REG} (green), or T_{FR} (red) from a single animal. (B) Expression in FPKM of select T_{FH} and T_{REG} genes in sorted populations from uninfected RM. (C) Heat map of log 2 transformed gene expression of transcripts in FPKM. Transcripts represent T_{FH} and T_{REG} signature genes. The T_{FH} gene signature was defined as transcripts that were significantly differentially expressed in sorted T_{FH} compared to bulk $CD4^+$ T-cells. T_{REG} gene signature was defined

as genes that were significantly differentially expressed in sorted T_{REG} compared to bulk $CD4^+$ T-cells. (D) Expression pattern of key T_{FH} and T_{REG} genes in sorted bulk $CD4^+$ T-cell, T_{FH}, T_{FR} and T_{REG} populations.

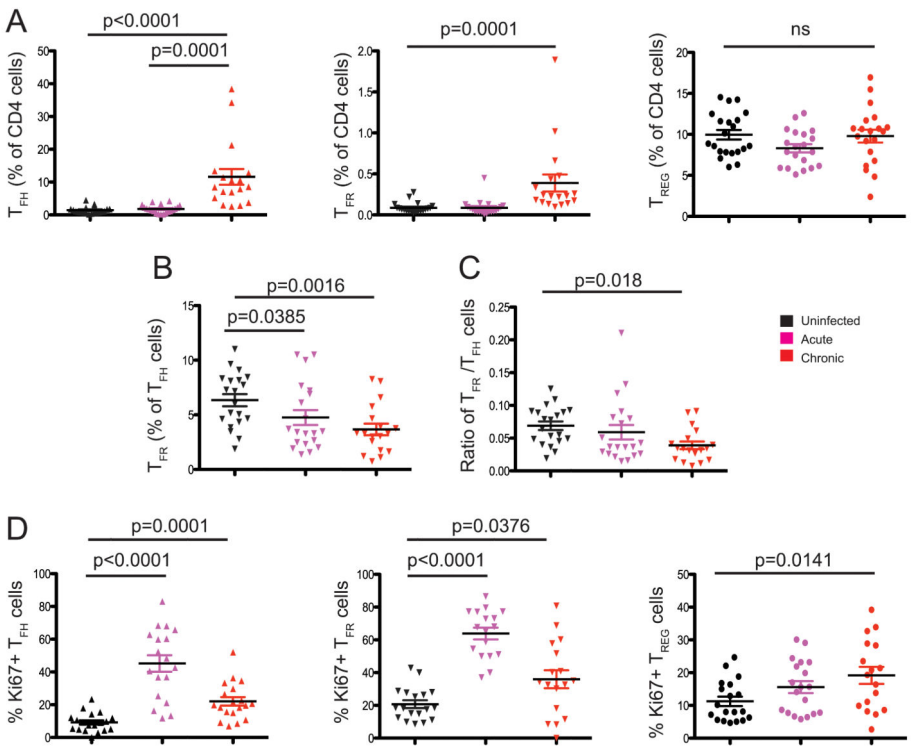

Figure 4. Kinetics of T_{FR}, T_{FH} and T_{REG} after SIV infection

(A) Frequency of T_{FH}, T_{FR} and T_{REG} as percentage of the total $CD4^+$ T-cell population within lymph nodes of uninfected, acutely (week 2) SIV-infected and chronically (week 24) SIV-infected RM. (B) Frequency of T_{FR} as a percent of T_{FH} within the lymph nodes of the same animals. (C) Ratio of frequencies of T_{FR} to the frequency of T_{FH} (both calculated as a percent of the total $CD4^+$ T-cell population). (D) Percent of proliferating, $Ki67^+$, T_{FH}, T_{FR} and T_{REG} within the lymph nodes of uninfected, acutely SIV-infected and chronically SIV-infected RM. Statistical analyses were performed using Mann-Whitney U tests.

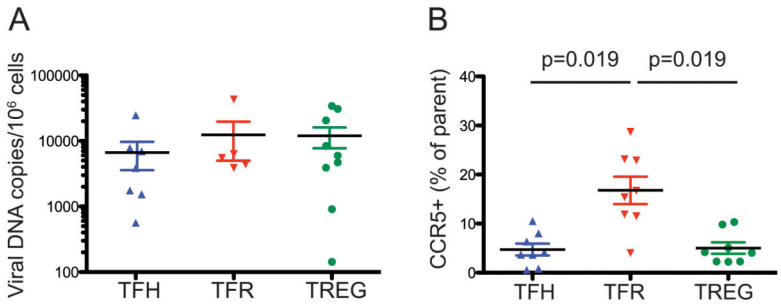

Figure 5. Comparable levels of SIV infection in T_{FH}, T_{FR} and T_{REG} isolated from the spleen of chronically SIV-infected RM

(A) Viral DNA copies per million sorted T_{FH}, T_{FR} and T_{REG} from spleens of unvaccinated chronically SIV-infected RM. (B) Percent of CCR5-expressing cells among T_{FH}, T_{FR} and T_{REG} in unvaccinated SIV-infected RM. Statistical analyses were performed using Mann-Whitney U tests.

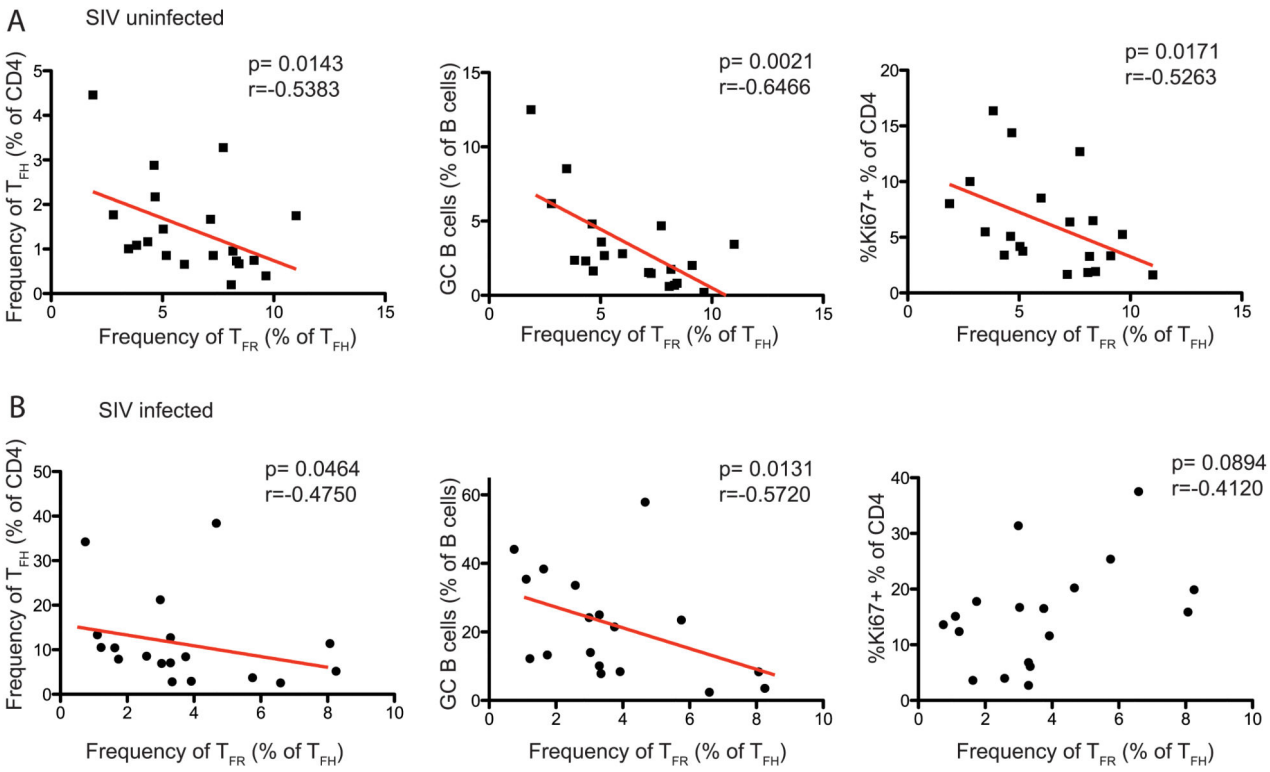

Figure 6. T_{FR} frequencies negatively correlate with T_{FH} and GC B-cell frequencies in the lymph nodes of RM

Correlations between the frequencies of T_{FR} (calculated as frequency of T_{FH}) and the frequencies of T_{FH} calculated as percent of total $CD4^+$ T-cells (left) and GC B-cells calculated as percent of total B-cells (center) and proliferating (i.e., $Ki67^+$) $CD4^+$ T-cells (right) within the lymph nodes of SIV-uninfected (A) and chronically SIV-infected (B) RM. Statistical analyses were performed using Spearman rank correlation tests.

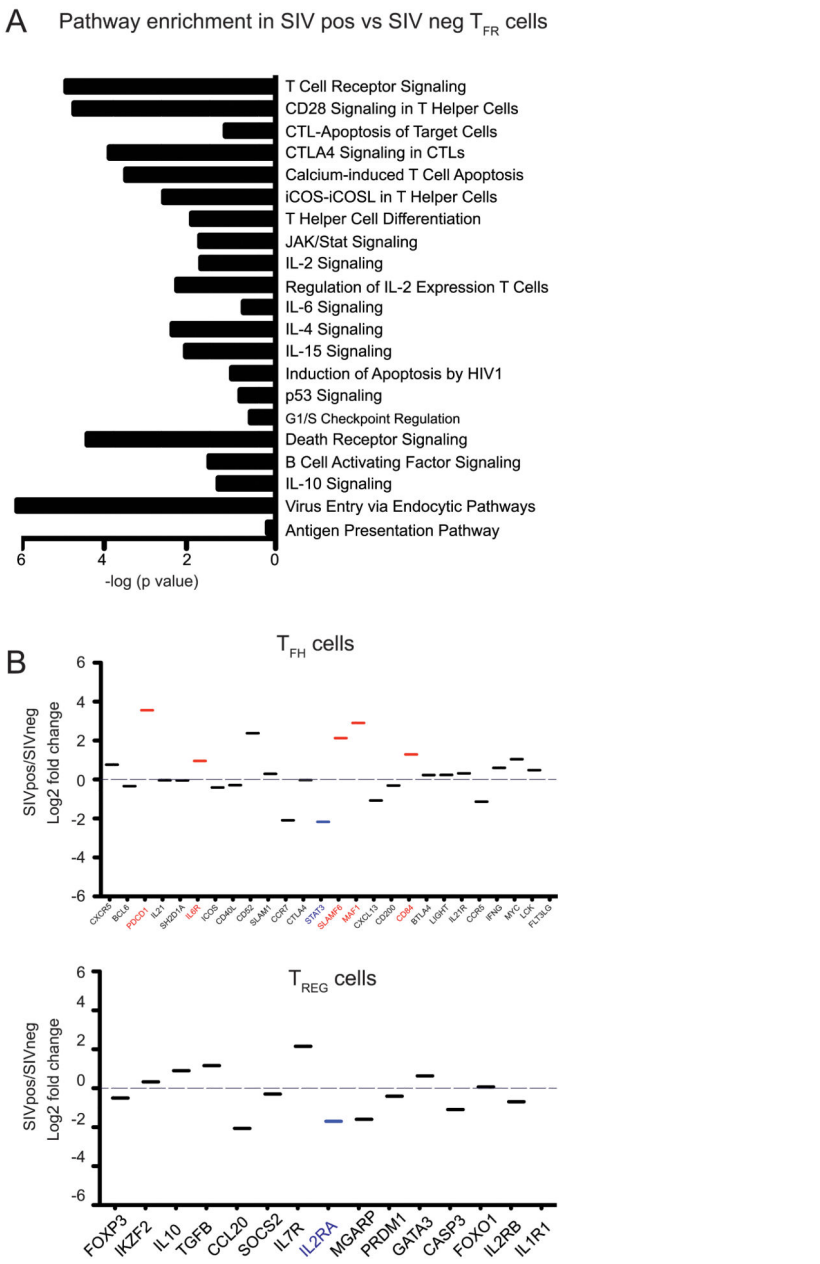

Figure 7. RNA expression within T_{FR} cells in uninfected and infected RM

(A) Enrichment of gene pathways in T_{FR} derived from the lymph nodes of unvaccinated SIV infected RM as compared to T_{FR} from SIV-uninfected animals as determined by Ingenuity Pathway Analysis. (B) Log 2 fold change of expression of T_{FH} and T_{REG} related gene transcripts in T_{FR} sorted from unvaccinated SIV-infected RM and SIV-uninfected RM. Significantly upregulated genes are in red and significantly down-regulated genes are in blue.